Improvement of the chromatic dispersion tolerance in coherent optical OFDM systems using shifted DFT windows for ultra-long-haul optical transmission systems

Minkyu Sung, [1] Hoon Kim,[2] Jaehoon Lee,[1] and Jichai Jeong[3,*]

[1]*Department of Computer and Radio Communication Engineering, Korea University, 145, Anam-ro, Sungbuk-ku, Seoul, 136-713, South Korea*

[2]*Department of Electrical & Computer Engineering, National University of Singapore, 4 Engineering Drive 3, Singapore 117583, Singapore*

[3]*Department of Brain and Cognitive Engineering, Korea University, 145, Anam-ro, Sungbuk-ku, Seoul, 136-713, South Korea*

[*]*jcj@korea.ac.kr*

Abstract: In a high-capacity ultra-long-haul optical coherent orthogonal frequency-division multiplexing (CO-OFDM) system, the dispersion tolerance is determined by the length of cyclic extension (CE). In this paper, we propose a novel scheme to substantially improve the dispersion tolerance of CO-OFDM systems without increasing the CE length. Multiple time-shifted discrete Fourier transform (DFT) windows are exploited at the receiver, each demodulating only a part of the subcarriers. Effectively, the proposed scheme reduces the bandwidth of the OFDM signals under demodulation. Numerical simulations are performed to show the improved dispersion tolerance of the proposed scheme in comparison with the conventional CO-OFDM system. We show that the dispersion tolerance improves by a factor equal to the number of DFT windows. The tradeoff between the improved dispersion tolerance and increased receiver complexity is also presented.

OCIS codes: (060.1660) Coherent communications; (060.2330) Fiber optics communications.

References and links

1. H. C. Bao and W. Shieh, "Transmission simulation of coherent optical OFDM signals in WDM systems," Opt. Express **15**(8), 4410–4418 (2007).
2. W. Shieh, H. Bao, and Y. Tang, "Coherent optical OFDM: theory and design," Opt. Express **16**(2), 841–859 (2008).
3. M. Sung, J. Lee, and J. Jeong, "DCT-precoding technique in optical fast OFDM for mitigating fiber nonlinearity," IEEE Photon. Technol. Lett. **25**(22), 2209–2212 (2013).
4. W. Shieh and I. Djordjevic, *OFDM for Optical Communications* (Academic Press, 2009).
5. X. W. Yi, W. Shieh, and Y. R. Ma, "Phase noise effects on high spectral efficiency coherent optical OFDM transmission," J. Lightwave Technol. **26**(10), 1309–1316 (2008).
6. H. Taga, "A theoretical study of OFDM system performance with respect to subcarrier numbers," Opt. Express **17**(21), 18638–18642 (2009).
7. Y. Ha and W. Chung, "Non-data-aided phase noise suppression scheme for CO-OFDM systems," IEEE Photon. Technol. Lett. **25**(17), 1703–1706 (2013).
8. M. Sung, S. Y. Kang, J. Shim, J. Lee, and J. Jeong, "DFT-precoded coherent optical OFDM with Hermitian symmetry for fiber nonlinearity mitigation," J. Lightwave Technol. **30**(17), 2757–2763 (2012).
9. Y. London and D. Sadot, "Nonlinear effects mitigation in coherent optical OFDM system in presence of high peak power," J. Lightwave Technol. **29**(21), 3275–3281 (2011).
10. S. J. Cao, P. Y. Kam, and C. Y. Yu, "Decision-aided, pilot-aided, decision-feedback phase estimation for coherent optical OFDM Systems," IEEE Photon. Technol. Lett. **24**(22), 2067–2069 (2012).
11. M. E. Mousa-Pasandi and D. V. Plant, "Non-iterative interpolation-based partial phase noise ICI mitigation for CO-OFDM transport systems," IEEE Photon. Technol. Lett. **23**(21), 1594–1596 (2011).

#214919 - $15.00 USD Received 1 Jul 2014; revised 17 Aug 2014; accepted 12 Sep 2014; published 18 Sep 2014

12. D. J. F. Barros and J. M. Kahn, "Optimized dispersion compensation using orthogonal frequency-division multiplexing," J. Lightwave Technol. **26**(16), 2889–2898 (2008).
13. X. Liu and F. Buchali, "Intra-symbol frequency-domain averaging based channel estimation for coherent optical OFDM," Opt. Express **16**(26), 21944–21957 (2008).
14. Y. Qi, T. Yan, M. Yiran, and W. Shieh, "Experimental demonstration and numerical simulation of 107-Gb/s high spectral efficiency coherent optical OFDM," J. Lightwave Technol. **27**(3), 168–176 (2009).
15. X. Liu, S. Chandrasekhar, B. Zhu, P. J. Winzer, A. H. Gnauck, and D. W. Peckham, "448-Gb/s reduced-guard interval CO-OFDM transmission over 2000 km of ultra-large-area fiber and five 80-GHz-grid ROADMs," J. Lightwave Technol. **29**(4), 483–490 (2011).
16. C. Chen, Q. Zhuge, and D. V. Plant, "Zero-guard-interval coherent optical OFDM with overlapped frequency-domain CD and PMD equalization," Opt. Express **19**(8), 7451–7467 (2011).
17. A. Tolmachev and M. Nazarathy, "Filter-bank based efficient transmission of reduced-guard-interval OFDM," Opt. Express **19**(26), B370–B384 (2011).
18. X. Yi and K. Qiu, "Estimation and compensation of sample frequency offset in coherent optical OFDM systems," Opt. Express **19**(14), 13503–13508 (2011).
19. W. Shieh and C. Athaudage, "Coherent optical orthogonal frequency division multiplexing," Electron. Lett. **42**(10), 587–589 (2006).
20. L. Tomba, "On the effect of Wiener phase noise in OFDM systems," IEEE Trans. Commun. **46**(5), 580–583 (1998).
21. G. P. Agrawal, *Nonlinear Fiber Optics* (Academic 1989).
22. C. Zhao and R. Baxley, "Error vector magnitude analysis for OFDM systems," in *Proceedings of Asilomar Conference on Signals, Systems, and Computers (ACSSC)*, pp. 1830–1834, (2006).
23. R. Shafik, S. Rahman, and A. R. Islam, "On the extended relationships among EVM, BER and SNR as performance metrics," in *Proceedings of International Conference on Electrical and Computer Engineering (ICECE)*, pp. 408–411, (2006).

1. Introduction

Coherent optical orthogonal frequency-division multiplexing (CO-OFDM) systems have recently received a great deal of attention as a transmission technology for high-capacity long-haul optical transport networks [1–3]. Compared to single-carrier-based systems, they provide fine granularity, flexible oversampling rate, simple one-tap equalization, and large dispersion tolerance [4]. These benefits are closely related to multi-carrier modulation of OFDM and thus typically obtained when the number of subcarriers is large. However, a large number of subcarriers impose other problems such as high peak-to-average power ratio (PAPR) of the OFDM signals and high susceptibility to the laser phase noise [5–7]. The large power variation of a high-PAPR signal not only requires a wide dynamic range of digital-to-analog converters (DACs) and analog-to-digital converters (ADCs) in the OFDM transceivers but it also makes the OFDM signal vulnerable to fiber nonlinearities [8, 9]. Optical OFDM signals with a large number of subcarriers should also be generated and detected by using narrow-linewidth transmitter and local oscillator (LO) lasers, respectively, to maintain a constant carrier phase during detection over a long symbol duration [10, 11]. Therefore, there exists an optimum number of subcarriers, N_c, to achieve the best performance, depending upon the system configurations and requirements.

On the other hand, the cyclic extension (CE) is inserted at the beginning, end, or both ends of OFDM symbols to combat the delay spread of the channel [12]. By setting the length of the CE larger than the delay spread, the OFDM receiver can recover the signals without suffering from inter-symbol interference (ISI) and inter-carrier interference (ICI). In high-capacity ultra-long-haul fiber-optic communication systems, fiber chromatic dispersion mainly determines the delay spread, which manifests itself as a time delay of each subcarrier in inverse proportion to its optical frequency. Thus, the length of the CE should be larger than the accumulated fiber dispersion times the bandwidth of the OFDM signal. However, since the CE is an overhead required to fight the fiber dispersion in CO-OFDM systems, its length should be minimized to maximize the spectral efficiency of the systems. This is especially so in high-capacity ultra-long-haul CO-OFDM systems where fiber dispersion is not periodically compensated at the amplifier sites and thus the OFDM signal experiences a significant amount of accumulated fiber dispersion. Nevertheless, under the aforementioned restriction of the number of subcarriers, the CE accounts for a non-negligible percentage of the symbol

#214919 - $15.00 USD Received 1 Jul 2014; revised 17 Aug 2014; accepted 12 Sep 2014; published 18 Sep 2014

duration in conventional CO-OFDM systems. For example, in the previously reported long-haul (e.g., >1000 km) CO-OFDM systems, the CE has occupied 10~25% of the symbol duration, which implies that the same percentage of the spectral efficiency should be sacrificed to cope with fiber dispersion [13, 14].

Recently, the reduced-guard-interval (RGI) and zero-guard-interval OFDM systems have been proposed to dramatically reduce the CE length or completely eliminate the CE in the OFDM symbols without their performance being affected by fiber dispersion [15, 16]. They both utilize overlapped frequency-domain equalizers (OFDEs) before OFDM demodulation at the receiver to compensate for the accumulated fiber dispersion in the similar manner as single-carrier systems do. However, the equalization-based dispersion compensation not only requires prior knowledge of the exact amount of accumulated dispersion to be compensated but it also greatly increases the computational complexity of the receiver.

In this paper, we propose a novel scheme for dramatically reducing the CE length of CO-OFDM systems or alternatively improving the dispersion tolerance of the systems when the CE length is fixed. We exploit multiple time-shifted discrete Fourier transform (DFT) windows to reduce the effective bandwidth of the OFDM signals under processing. Therefore, the proposed coherent optical shifted-DFT window OFDM (CO-SDW-OFDM) system substantially improves the dispersion tolerance by a factor equal to the number of DFT windows. Multiple DFT blocks can be readily implemented by using a fast Fourier transform (FFT) algorithm. Compared to the multi-sub-bands OFDM system where OFDM subcarriers are separated into multiple sub-bands using digital filter banks [17], the proposed CO-SDW-OFDM system does not suffer from non-orthogonality between subcarriers caused by non-ideal filtering of subcarriers since our system separates the OFDM subcarriers in the time domain through shifted DFT windows.

The remainder of this paper is organized as follows. The operation principles of the proposed scheme along with its mathematical expression are explained in Section 2. The setup for numerical simulations and the performance of the proposed scheme in comparison with conventional OFDM systems are described in Section 3. Finally, Section 4 summarizes this paper.

2. Operation principles of the proposed CO-SDW-OFDM system

Figure 1 illustrates exemplary waveforms of the transmitted and received OFDM signals. As shown in Fig. 1(a), the modulated OFDM signal is multiplexed with multiple subcarriers, each carrying the data symbol including quadrature amplitude modulation (QAM) signals. The CE is inserted at both ends of the symbol in this example to combat the chromatic dispersion [12]. After transmission over dispersive fiber, each subcarrier experiences different time delays which increase in inverse proportion to optical frequency of the subcarrier. When the delay spread is shorter than the CE length as shown in Fig. 1(b), the symbol transitions do not intrude into the DFT window and neither ISI nor ICI occurs during demodulation. On the other hand, when the delay spread is longer than the CE length as shown in Fig. 1(c), the transmission performance will be degraded by ISI and ICI.

#214919 - $15.00 USD Received 1 Jul 2014; revised 17 Aug 2014; accepted 12 Sep 2014; published 18 Sep 2014

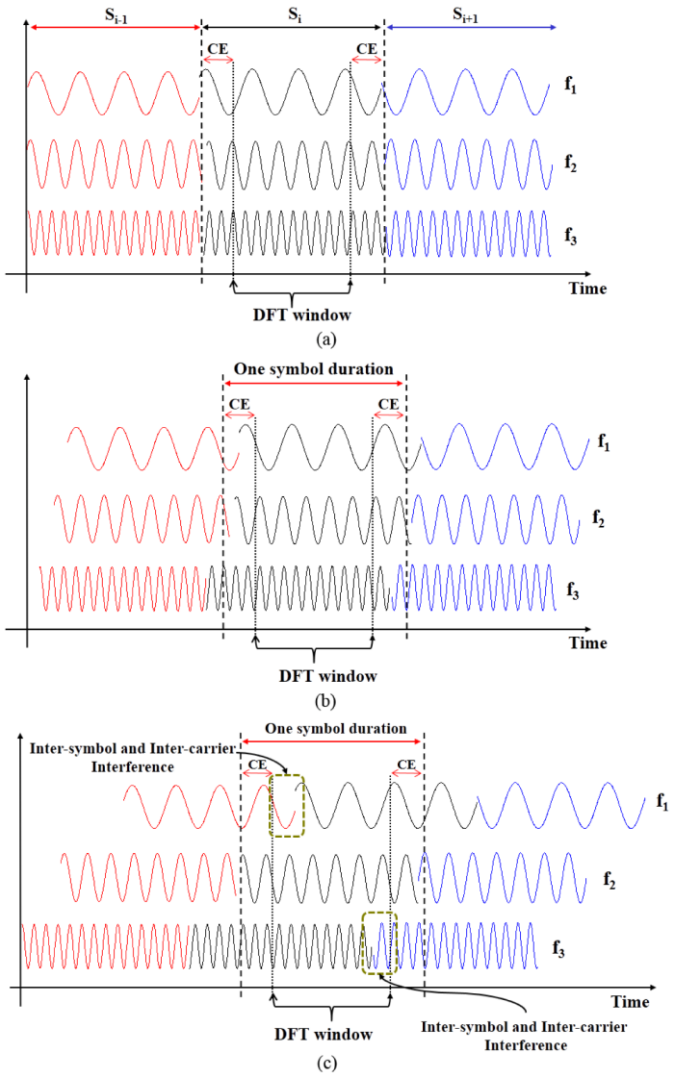

Fig. 1. Transmitted and received OFDM signals: (a) transmitted signal, (b) received signal at channel length shorter than cyclic extension length, and (c) received signal at channel length longer than cyclic extension length where $f_1 < f_2 < f_3$.

We propose the time-shifted DFT window OFDM system to improve the chromatic dispersion tolerance without increasing the CE length. For simplicity of explanation, we employ only two shifted DFT windows in this section: lower-side DFT (LS-DFT) window and upper-side (US-DFT) window at the receiver, as shown in Fig. 2. Compared to the conventional DFT window, the US-DFT window advances over the conventional window in time whereas the lower-side one is delayed. Since each shifted DFT windows demodulates all the subcarriers simultaneously, we have two differently demodulated subcarriers from the two DFT blocks. Among the two sets of demodulated subcarriers, some subcarriers suffer from ISI. Thus, we can select the subcarriers from both the DFT blocks to make a new single set of subcarriers which are all free from the ISI. Since chromatic dispersion simply delays the subcarriers in proportion to its optical wavelength (or in inverse proportion to its optical frequency), we should select the half of the low-frequency subcarriers from the LS-DFT block while the other half of the high-frequency subcarriers from the US-DFT block. For

#214919 - $15.00 USD Received 1 Jul 2014; revised 17 Aug 2014; accepted 12 Sep 2014; published 18 Sep 2014

example, two subcarriers at frequency f_1 and f_3 suffer from ISI in the conventional CO-OFDM in Fig. 3(a) but only the subcarrier at f_3 has symbol transitions within the LS-DFT window in Fig. 3(b) and thus suffers from ISI. On the other hand, we have an ISI-free subcarrier at f_3 from the output of US-DFT block. Thus, we can demodulate all the subcarriers free from ISI by selecting f_1 and f_2 subcarriers from the LS-DFT block and f_3 subcarrier from the US-DFT block. Note that ICI is a crosstalk between subcarriers arising from loss of orthogonality of particular subcarriers. However, it is remained for the proposed system although ISI is perfectly removed. For example, when we obtain f_3 subcarrier from the US-DFT block, f_1 subcarrier leads to ICI for f_2 and f_3 subcarriers in demodulation of OFDM signals, although the ISI of f_3 subcarrier can be perfectly removed. However, the ICI coefficients are different according to the distance between required subcarrier and the subcarrier occurring ICI [18]. Therefore, the ICI coefficient of f_3 subcarrier is smaller that of f_2 subcarrier. In other words, the proposed system can reduce the ICI coefficient at f_3 subcarrier by increasing the distance from ICI-leading subcarriers and removing ICI resulting from f_3 subcarrier. In case of f_2 subcarrier, the conventional systems suffer from ICI due to f_1 and f_3 subcarriers. On the other hand, the proposed system only suffers from ICI due to only f_1 subcarrier. As a result, we can also reduce ICI in the proposed system.

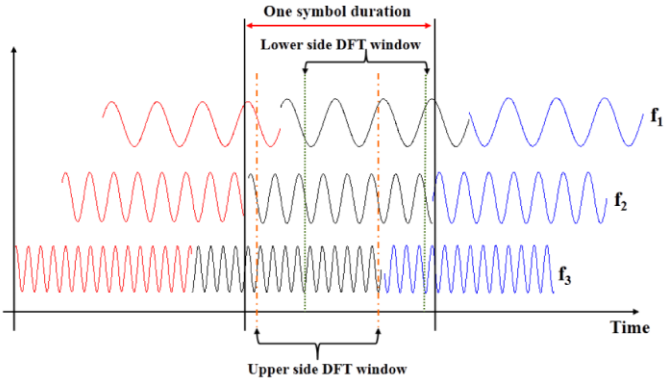

Fig. 2. Received signals in the proposed CO-SDW-OFDM where $f_1 < f_2 < f_3$.

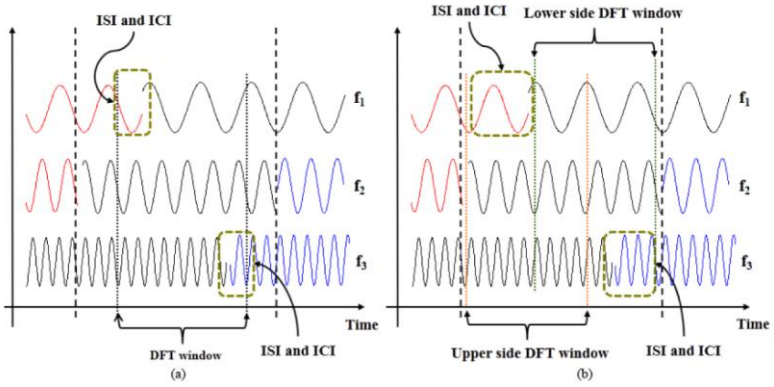

Fig. 3. Received signals of the conventional CO-OFDM and proposed CO-SDW-OFDM systems in one symbol duration for comparison: (a) conventional CO-OFDM system and (b) proposed CO-SDW-OFDM system where $f_1 < f_2 < f_3$.

#214919 - $15.00 USD Received 1 Jul 2014; revised 17 Aug 2014; accepted 12 Sep 2014; published 18 Sep 2014

2.1 Mathematical expression of the conventional OFDM system

At the transmitter, let $S_k = [S_0, S_1, \ldots, S_{Nc-1}]^T$, where N_c is the size of IFFT, be the input signal vector with each scalar complex quantity representing modulated data. The transmitted signal in the time domain is then expressed as

$$s_i(\tau) = \frac{1}{\sqrt{N_c}} \sum_{k=0}^{N_c-1} S_k \cdot e^{j2\pi \frac{k}{N_c}\tau}, \ (0 \le \tau \le N_c - 1) \tag{1}$$

At the receiver, assuming that the delay spread exceeds the CE length, the received signal of the conventional CO-OFDM system can be expressed as

$$y_i(\tau) = r_i(\tau) + n_i(\tau), \quad (0 \le \tau \le N_c - 1) \tag{2}$$

and

$$r_i(\tau) = \begin{cases} \underbrace{\sum_{r=N_{CE}/2+1}^{L_p-1} s_{i-1}(\tau + N_c + 3\times N_{CE}/2 - r)\cdot h_{channel}(r)}_{ISI} \\ \quad - \underbrace{\sum_{n=N_{CE}/2+1}^{L_p-1} s_i(\tau + N_c + 3\times N_{CE}/2 - n)\cdot h_{channel}(n)}_{ICI} + \sum_{q=0}^{N_c-1} s_i(\tau - q)\cdot h_{channel}(q) \quad (0 \le \tau \le L_p - 1) \\ \sum_{r=0}^{N_c-1} s_i(\tau - r)\cdot h_{channel}(r) \quad (L_p \le \tau \le N_c - L_n - 1) \\ \underbrace{\sum_{r=-L_n+1}^{-N_{CE}/2-1} s_{i+1}(\tau - N_c - N_{CE}/2 - r)\cdot h_{channel}(r)}_{ISI} \\ \quad - \underbrace{\sum_{n=-L_n+1}^{-N_{CE}/2-1} s_i(\tau - N_c - N_{CE}/2 - n)\cdot h_{channel}(n)}_{ICI} + \sum_{q=0}^{N_c-1} s_i(\tau - q)\cdot h_{channel}(q) \quad (N_c - L_n \le \tau \le N_c - 1) \end{cases} \tag{3}$$

where $n_i(\tau)$ denotes the additive white Gaussian noise (AWGN) generated from optical amplifiers on the link, N_{CE} is the CE length, and the L_p and L_n are the positive and negative lengths of channel impulse response caused by dispersion, respectively. Equation (3) clearly shows that when the channel delay spread is longer than the CE length, both ISI and ICI occur at the receiver and interfere with the data symbols. These interferers cannot be easily compensated by electrical equalization at the receiver and thus can limit the transmission performance of the conventional CO-OFDM system.

2.2 Mathematical expression of proposed CO-SDW-OFDM system

For the proposed CO-SDW-OFDM system, the received signal expressed in Eq. (2) is split two and each fed to two time-shifted FFT blocks. Then the outputs of the FFT blocks can be written as following:

#214919 - $15.00 USD Received 1 Jul 2014; revised 17 Aug 2014; accepted 12 Sep 2014; published 18 Sep 2014

$$y^{upper}{}_i(\tau)=\begin{cases}\sum_{q=0}^{N_c-1} s_i(\tau-q)\cdot h_{upper}(q) \;+\; \underbrace{\sum_{r=N_{CE}/2+1}^{L_p+m-1} s_{i-1}(\tau+N_c+3\times N_{CE}/2-r)\cdot h_{upper}(r)}_{ISI} \\ \qquad -\underbrace{\sum_{n=N_{CE}/2+1}^{L_p+m-1} s_i(\tau+N_c+3\times N_{CE}/2-n)\cdot h_{upper}(n)}_{ICI} \qquad (0\le\tau\le N_c-1)\end{cases} \tag{4}$$

$$y^{lower}{}_i(\tau)=\begin{cases}\sum_{q=0}^{N_c-1} s_i(\tau-q)\cdot h_{lower}(q)+\underbrace{\sum_{r=-L_n-m+1}^{-N_{CE}/2-1} s_{i+1}(\tau-N_c-N_{CE}/2-r)\cdot h_{lower}(r)}_{ISI} \\ \qquad -\underbrace{\sum_{n=-L_n-m+1}^{-N_{CE}/2-1} s_i(\tau-N_c-N_{CE}/2-n)\cdot h_{lower}(n)}_{ICI} \qquad (0\le\tau\le N_c-1)\end{cases} \tag{5}$$

where m is the shift factor and can be expressed as

$$\frac{4m}{f_s}=\frac{c}{f_c^{\,2}}\cdot|D|\cdot N_{sc}\cdot\Delta f \tag{6}$$

and

$$m=\frac{1}{4}\cdot\frac{c}{f_c^{\,2}}\cdot|D|\cdot\frac{N_{sc}}{N_c}\cdot f_s^{\,2} \tag{7}$$

where f_c is the frequency of the unmodulated optical carrier, c is the speed of light, D is the accumulated dispersion in the unit of ps/pm, f_s is the sampling frequency, Δf is the subcarrier spacing, and N_{sc} is the number of data subcarriers. The right term of Eq. (6) is the delay spread due to chromatic dispersion between the center subcarrier and edge subcarriers [19]. Although shifted DFT windows are used in Eqs. (4) and (5), the ISI and ICI terms still exist. However, when the sum of CE length and the shifted length of DFT window (m) exceeds the channel delay spread, the ISI and ICI distortions occur only at some particular subcarriers, as shown in Fig. 3(b). Therefore, y^{upper} and y^{lower} after FFT operation can be expressed as

$$Y^{upper}{}_i(k)=\sum_{\tau=0}^{N_c-1} y^{upper}{}_i(\tau)\cdot e^{-j2\pi\frac{\tau}{N_c}k},\ (0\le k\le N_c-1) \tag{8}$$

$$Y^{lower}{}_i(k)=\sum_{\tau=0}^{N_c-1} y^{lower}{}_i(\tau)\cdot e^{-j2\pi\frac{\tau}{N_c}k},\ (0\le k\le N_c-1) \tag{9}$$

and

#214919 - $15.00 USD Received 1 Jul 2014; revised 17 Aug 2014; accepted 12 Sep 2014; published 18 Sep 2014

$$Y^{upper}{}_i(k)=\begin{cases} S_i(k)\cdot H_{upper}(k) & (0\le k\le N_c/2-1) \\ S_i(k)\cdot H_{upper}(k)+\underbrace{\sum_{\tau=0}^{N_c-1}\left(\sum_{r=N_{CE}/2+1}^{L_p+m-1} s_{i-1}(\tau+N_c+3\times N_{CE}/2-r)\cdot h_{upper}(r)\right)e^{-j2\pi\frac{\tau}{N_c}k}}_{ISI_{upper}(k)} & \\ \underbrace{-\sum_{\tau=0}^{N_c-1}\left(\sum_{n=N_{CE}/2+1}^{L_p+m-1} s_i(\tau+N_c+3\times N_{CE}/2-n)\cdot h_{upper}(n)\right)e^{-j2\pi\frac{\tau}{N_c}k}}_{ICI_{upper}(k)} & (N_c/2\le k\le N_c-1) \end{cases} \tag{10}$$

$$Y^{lower}{}_i(k)=\begin{cases} S_i(k)\cdot H_{lower}(k)+\underbrace{\sum_{\tau=0}^{N_c-1}\left(\sum_{r=-L_n-m+1}^{-N_{CE}/2-1} s_{i+1}(\tau-N_c-N_{CE}/2-r)\cdot h_{lower}(r)\right)e^{-j2\pi\frac{\tau}{N_c}k}}_{ISI_{lower}(k)} & \\ \underbrace{-\sum_{\tau=0}^{N_c-1}\left(\sum_{n=-L_n-m+1}^{-N_{CE}/2-1} s_i(\tau-N_c-N_{CE}/2-n)\cdot h_{lower}(n)\right)e^{-j2\pi\frac{\tau}{N_c}k}}_{ICI_{lower}(k)} & (0\le k\le N_c/2-1) \\ S_i(k)\cdot H_{lower}(k) & (N_c/2\le k\le N_c-1) \end{cases} \tag{11}$$

The received subcarriers after the FFT operation can be re-organized to remove the ISI term as

$$Y_i(k)=\begin{cases} Y^{upper}{}_i(k), & (0\le k\le N_c/2-1) \\ Y^{lower}{}_i(k), & (N_c/2\le k\le N_c-1) \end{cases} \tag{12}$$

For Eqs. (8) and (9), the required additional processing to implement the CO-SDW-OFDM system is just additional FFT operation.

3. Simulation and results

3.1 Simulation setup

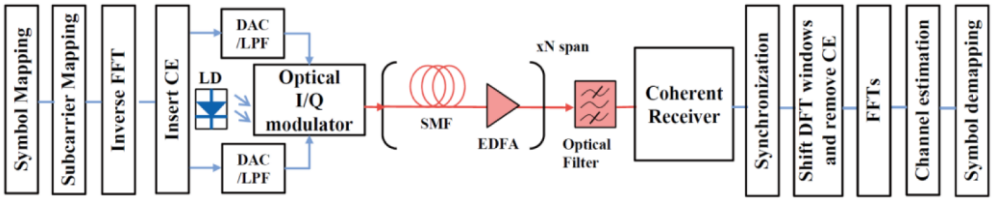

Fig. 4. Simulation configuration of the proposed CO-SDW-OFDM system.

To investigate the transmission performances of the proposed CO-SDW-OFDM system, we carry out numerical simulations of the system depicted in Fig. 4. A pseudo-random binary sequence is first converted into numerous parallel data to be each mapped onto the 4-QAM signal before sending them to the IFFT block. The sizes of IFFT used in our simulation are 128, 256, 512 and 1024. Only the half of the subcarriers in the IFFT input carry the modulated data and the remaining subcarriers are zero-padded for oversampling and guard

#214919 - $15.00 USD Received 1 Jul 2014; revised 17 Aug 2014; accepted 12 Sep 2014; published 18 Sep 2014

band. We add a CE to the OFDM symbols to combat the fiber dispersion. Also inserted in the OFDM symbols are training and pilot symbols to estimate the channel information and to compensate for the laser phase noise, respectively. The two overheads occupy 5% of the symbol duration each. The generated OFDM signals are then converted to analog signals using DACs with a sampling rate of 20 Gsample/s to drive an optical I/Q modulator. Thus, the largest net data rate of the OFDM signal becomes 18 Gb/s (= $20 \times \log_2 4 \times 0.5 \times 0.90$), occupying approximately 10 GHz of bandwidth. The net data rate should decrease as much as the CE is added. The laser diode which generates continuous wave light is modeled to have phase noise governed by the Wiener process [20]. The transmission link is composed of multi-spans of an 80-km standard single-mode fiber (SSMF) and an erbium-doped fiber amplifier (EDFA) which exactly compensates for the loss of each SSMF span. The EDFA has a noise figure of 6 dB. The SSMF has a dispersion coefficient of 17 ps/nm/km, a dispersion slope of 0.05936 ps/nm^2/km, a nonlinear index of 1.3 W^{-1}km^{-1}, an effective core area of 78 μm^2, and an attenuation coefficient of 0.2 dB/km. The split-step Fourier method is used to solve the nonlinear Schrödinger equation which describes the wave propagation along the single-mode fiber [21]. At the receiver, the optical OFDM signal is detected by an optical coherent detector, which consists of an LO laser, an optical 90° hybrid, and two balanced detectors. After timing synchronization, the OFDM signal of the proposed system is demodulated by multiple time-shifted FFTs whereas the conventional OFDM system utilizes a single FFT block. Then, the zero-forcing equalization is performed based on channel estimation using the training symbols. Common phase error correction is also performed using the pilot subcarriers before the decision is made for each subcarrier symbol to finally evaluate the system performance.

3.2 Dispersion tolerance

The transmission performance of the 4-QAM-modulated OFDM system is evaluated by using the error vector magnitude (EVM) [22]. Two DFT windows are used for the proposed CO-SDW-OFDM signal in this subsection and the effects of the number of DFT windows on the system performance are discussed in subsection 3.3. Figure 5 shows the EVMs of the proposed CO-SDW-OFDM signal as a function of the accumulated fiber dispersion for various different lengths of the CE. Also shown in the figure is the EVM performance of the conventional CO-OFDM system. The FFT size used in this simulation is set to be 256 and the OSNR is fixed at 15 dB. The laser linewidth is assumed to be 0 Hz to focus primarily on the dispersion tolerance for different CE lengths. The CE ratio is defined as the length ratio between the CE and symbol. The figure shows that we have an EVM of 13% at the back-to-back operation (i.e., in the absence of chromatic dispersion), the performance of which is determined by the OSNR. The figure also shows that the delay spread induced by fiber dispersion would not deteriorate the performance of the conventional OFDM system as long as the CE is longer than the spread. For example, the conventional OFDM system having a CE ratio of 1/8 exhibits negligible EVM penalties until the fiber dispersion is accumulated up to 20000 ps/nm [= 256/8/20 ns (CE length) ÷ 0.08 nm (spectral width)]. Thus, the dispersion tolerance of the conventional CO-OFDM system shrinks as the CE length is reduced. On the other hand, the proposed CO-SDW-OFDM system has a doubled dispersion tolerance compared to the conventional CO-OFDM system. This is because each shifted DFT block demodulates the half of the OFDM subcarriers and thus halves the effective bandwidth of the signal under demodulation. The simulation results show that the proposed system with a CE ratio of merely 1/64 can achieve an EVM of 28%, which corresponds to a bit-error rate of 10^{-3} for AWGN-limited systems [23], over 3000-km SSMF without any dispersion compensation.

#214919 - $15.00 USD Received 1 Jul 2014; revised 17 Aug 2014; accepted 12 Sep 2014; published 18 Sep 2014

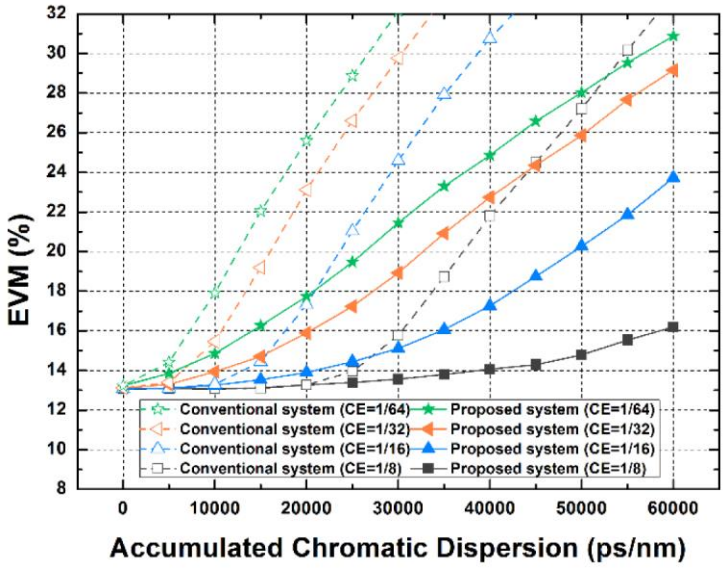

Fig. 5. EVM performances as a function of accumulated chromatic dispersion for different cyclic extension ratios. FFT size = 256.

Next, we investigate the impact of FFT size and laser phase noise on the dispersion tolerance of the proposed CO-SDW-OFDM system. Figure 6 shows the EVM performance as a function of the accumulated chromatic dispersion for the FFT sizes of 128, 256, 512, and 1024. The length of the CE is fixed to be 1/16 of the symbol duration. Four different laser linewidths, 0, 100, 200, 300, and 400 kHz are used to plot Figs. 6(a)-6(d), respectively. The OFDM system having a large FFT size clearly exhibits better dispersion tolerance since the CE length is proportional to the symbol duration in this plot (note that the CE ratio is fixed to be 1/16). Comparing the dispersion tolerance between the two OFDM systems, the conventional CO-OFDM system behaves similar to the CO-SDW-OFDM system with half the FFT size in the absence of laser phase noise. For example, both the conventional CO-OFDM system with 1024 FFT size and the CO-SDW-OFDM system with 512 FFT size show an EVM of 18% at the accumulated dispersion of 80000 ps/nm. As the laser linewidth increases, however, the conventional CO-OFDM system starts to underperform the CO-SDW-OFDM system having half the FFT size, as shown in Figs. 6(b)-6(d). This should be ascribed to the fact that the large-FFT-size OFDM system is susceptible to laser phase noise. A chance of carrier phase fluctuating within a long symbol duration increases with the laser linewidth. The results show that the proposed system can reduce the FFT size by half while achieving better dispersion tolerance than the conventional OFDM system. It should be noted that the reduced FFT size also brings benefits such as low PAPR and resilience to laser phase noise and frequency offset between the transmitter and LO lasers.

#214919 - $15.00 USD Received 1 Jul 2014; revised 17 Aug 2014; accepted 12 Sep 2014; published 18 Sep 2014

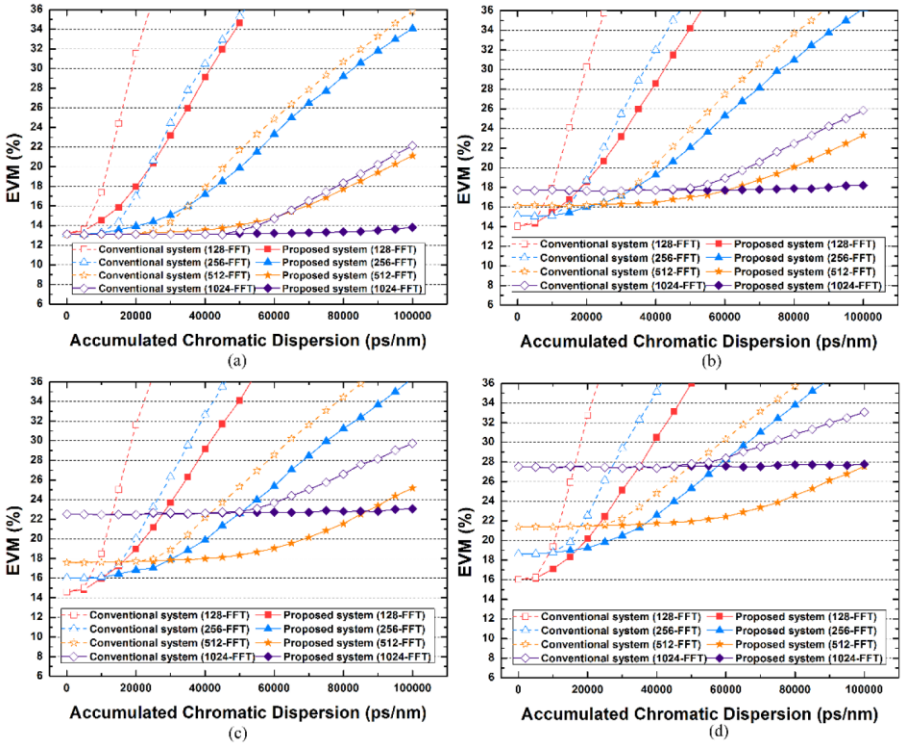

Fig. 6. EVM performances as a function of accumulated chromatic dispersion for the different FFT sizes and laser phase noises with laser linewidths: (a) 0 kHz, (b) 100 kHz, (c) 200 kHz, and (d) 400 kHz.

3.3 Effects of the number of shifted DFT windows on the system complexity and transmission performance

The improved dispersion tolerance of the proposed CO-SDW-OFDM system comes from the fact that a shifted DFT window discards the subcarriers which suffer from ISI and thus reduces the effective bandwidth of the OFDM signal demodulated. Therefore, the dispersion tolerance of the proposed CO-SDW-OFDM system is further improved as the number of shifted DFT windows, k, increases. Alternatively, the CE length can be reduced by a factor of the number of DFT windows when the FFT size of the OFDM signal is fixed. However, these benefits come at the expense of the receiver complexity, i.e., more FFT blocks at the receiver. The number of complex multiplications per bit in an FFT block is calculated as

$$\frac{N_c / 2 \times \log_2 N_c}{N_{sc} \times \log_2 M} \tag{13}$$

where M is the modulation order. If the FFT size is 256, M equals to 4, and N_c/N_{sc} is 2, the complex multiplications per bit become 4 and $4k$ for the conventional CO-OFDM and CO-SDW-OFDM systems, respectively. Figure 7 shows the dispersion tolerance as a function of the number of shifted DFT windows. The FFT size is fixed to 256 and the deleterious effect of laser phase noise is not included. The target EVM is 28% and the OSNR of the signal is set to be 15 dB. Figure 7 shows that the dispersion tolerance increases almost linearly with the number of shifted DFT windows. For example, we achieve the improvement of dispersion tolerance by a factor of 4.0~4.1 when four shifted DFT blocks are employed at the receiver, compared to the conventional CO-OFDM which utilizes a single DFT block. In this case,

#214919 - $15.00 USD Received 1 Jul 2014; revised 17 Aug 2014; accepted 12 Sep 2014; published 18 Sep 2014

however, the number of complex multiplication required for the demodulation also increases by a factor of 4.

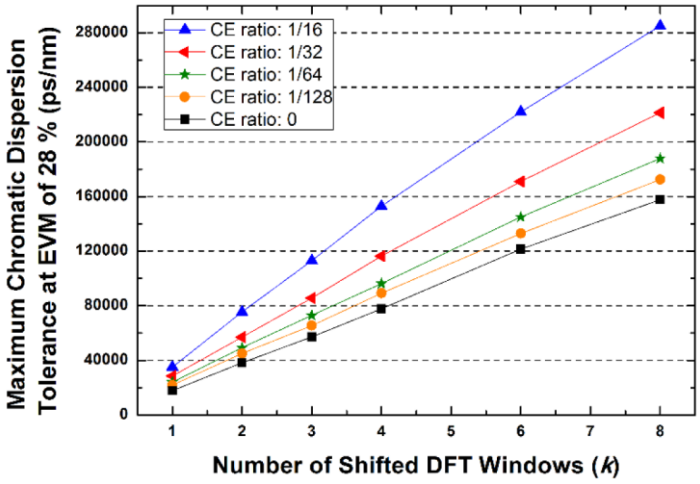

Fig. 7. Maximum chromatic dispersion tolerances at EVM of 28% as a function of the number of shifted DFT windows for various CE ratios of OFDM signal.

It is interesting to compare the implementation complexity of the proposed scheme with that of the RGI-OFDM system. The number of complex multiplications for the RGI-OFDM system can be written as

$$\frac{2\times(N_{OFDE}\times\log_2 N_{OFDE}+N_{OFDE})}{N_{sc}\times\log_2 M\times N_{OFDE}/N_c}+\frac{N_c/2\times\log_2 N_c}{N_{sc}\times\log_2 M} \tag{14}$$

where N_{OFDE} is the FFT size for OFDE operation. The first term in (14) is for OFDE processing and the second term is for FFT [16]. N_{OFDE} is typically larger than the number of subcarriers, N_c. Therefore, if N_{OFDE}/N_c is 16 as given in [16], the complex multiplication of the RGI-OFDM system can be calculated to be 30, which is larger than the case where we have 7 shifted DFT windows.

It is worth noting' that the maximum number of shifted DFT windows in the proposed scheme will be determined by the number of subcarriers, N_c. When the number of shifted DFT windows equals to N_c, each DFT window at the receiver will demodulate only one subcarrier, discarding N_c-1 subcarriers. As shown in previous simulation results, this will allow us to reduce the CE length by a factor of N_c or equivalently improves the dispersion tolerance by the same factor.

3.4 Transmission performance

Lastly, we investigate the maximum transmission distance of the proposed OFDM system. Figure 8 shows the EVM performance of the proposed scheme as a function of the transmission distance over SSMF, in comparison with the performance of the conventional CO-OFDM system. The FFT size, fiber launch power, and laser linewidth are set to be 256 points, −3 dBm, and 100 kHz, respectively. Thanks mainly to the superior dispersion tolerance, the proposed system outperforms the conventional CO-OFDM system. Furthermore, the performance improvement of the proposed system increases with the number of DFT windows. However, when a CE ratio of 1/16 is employed, the performance difference between k = 3 and 4 is marginal. This is because the transmission performance of the two proposed systems is not dominated by dispersion. Instead, other impairments such as fiber nonlinearity, laser phase noise, and ASE noise mainly limit the transmission

#214919 - $15.00 USD Received 1 Jul 2014; revised 17 Aug 2014; accepted 12 Sep 2014; published 18 Sep 2014

performance of the proposed system. The simulation result shows that the proposed CO-SDW-OFDM signal with no CE and 4 shifted windows can bridge up to 2400 km without any dispersion compensation. This is even longer than the maximum transmission distance of the conventional CO-OFDM system with a 1/16 CE ratio. Therefore, the proposed CO-SDW-OFDM system can improve the spectral efficiency by completely removing CE while having superior transmission performance to the conventional CO-OFDM system.

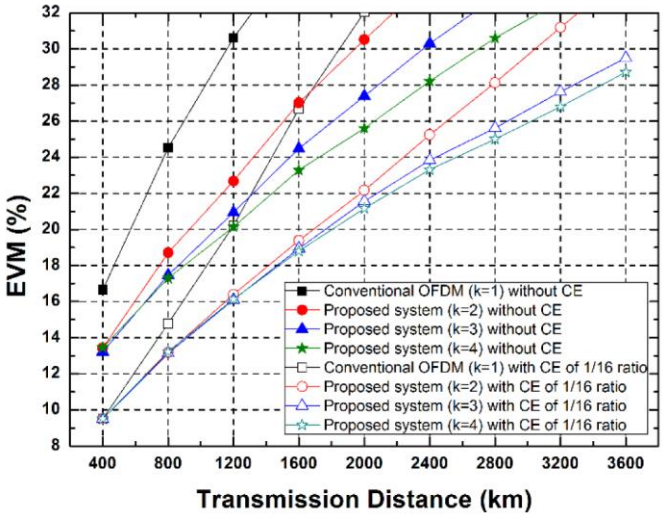

Fig. 8. EVM performances as a function of transmission distance of the conventional CO-OFDM and proposed CO-SDW-OFDM systems for different the number of shifted DFT windows (k).

4. Conclusions

We have proposed a novel coherent optical shifted DFT window OFDM system to improve the dispersion tolerance of the system without increasing the length of cyclic extension. The proposed scheme utilizes multiple time-shifted DFT windows to utilize a part of the demodulated subcarriers, which does not suffer from ISI and reduce ICI induced by accumulated fiber dispersion. Numerical simulation is performed to investigate the dispersion tolerance improvement over the conventional CO-OFDM system. It is shown that the dispersion tolerance of the proposed scheme increases by a factor equal to the number of shifted DFT windows, compared to the conventional CO-OFDM system. The 17.72 Gb/s CO-SDW-OFDM system using two shifted DFT windows achieves an EVM of <28% at the accumulated dispersion of 50000 ps/nm. However, this advantage comes at the expense of receiver complexity, i.e., more FFT blocks. Nevertheless, the proposed scheme is less complex than the reduced-guard-interval OFDM system which utilizes frequency-domain equalization to compensate for the dispersion at the receiver. Moreover, the proposed scheme does not require prior knowledge of exact amount of accumulated dispersion. We believe that the proposed CO-SDW-OFDM system can be easily extended to other CO-OFDM systems such as orthogonal-band-multiplexing OFDM to improve data rate up to Tb/s and DFT-spread OFDM systems to enhance nonlinear performance for the future ultra-long-haul optical transmission systems.

Acknowledgments

This work was supported by the Basic Science Research Program through the National Research Foundation of Korea funded by the Ministry of Education, Science and Technology under Grant 2013R1A1A2009689.